

USE OF AUGMENTED CONTINUUM THEORY FOR MODELING THE SIZE DEPENDENT MATERIAL BEHAVIOR OF NANO-ACTUATORS*

Y. TADI BENI

Faculty of Engineering, University of Shahrekord, Shahrekord, I. R. of Iran
Email: tadi@eng.sku.ac.ir

Abstract– In this paper, an augmented continuum mechanics is applied to investigate the size dependent pull-in instability of torsional nano-electromechanical actuator considering the coupling effect between torsion and bending. A set of dimensionless governing equations of the system is derived using the effective size dependent flexural and torsional rigidity of the actuator. The governing equations are solved using implicit function theorem. The static instability parameters i.e pull-in angle, pull-in displacement and pull-in voltage are computed as a function of bending/torsion coupling ratio as well as the actuator geometrical characteristics and size effect parameter. It is found that pull-in characteristics computed by the augmented continuum mechanics has a considerable difference with those predicted via classical theory when the dimensions of the nano-actuator are of the order of the internal material length scale parameter.

Keywords– Augmented continuum theory, electrostatic torsional actuator, pull-in instability, torsion/bending coupling

1. INTRODUCTION

For the past decade nanotechnology has greatly influenced all science and engineering branches including physics [1], electronics [2], civil engineering [3], material engineering [4] etc. In the electronic world, nano-electromechanical systems (NEMS) have become the center of interest for developing ultra-small devices. There are several kinds of NEMS actuated by electrostatic forces including flexural actuators as well as torsional actuators [5-7]. The schematic of an electrostatic torsional nano-actuator with two degree of freedom is shown in Fig. 1. A typical torsional nano-actuator is constructed from two conductive components in which one is movable and the other is fixed. The fixed component consists of two identical conductive electrodes which are fixed on a rigid substrate. The movable component is a conductive mainplate suspended by two nano-beams over the fixed component. The movable mainplate can be driven to rotate by applying voltage difference between the mainplate and one of the fixed electrodes, and can rotate in the reverse direction if potential is applied between the mainplate and another electrode. Interestingly, for long/thin enough nano-beams, electrostatic actuation can cause the movable component to deflect and rotate simultaneously. By increasing the applied voltage above a critical value, the electrostatic force/torque overcomes the mechanical ones and the mainplate deforms abruptly and pulls into the fixed ground electrode. Determining the pull-in parameters, i.e. pull-in voltage, angle, and deflection of a torsional actuator is crucial for design reliable ultra-small systems. The physical behavior of the torsional actuators has been extensively studied in micro scales [8-13]. Some researchers developed analytical lumped-mass models to simulate the pull-in performance of torsional micromirrors [9-11].

*Received by the editors September 21, 2011; Accepted January 18, 2012.

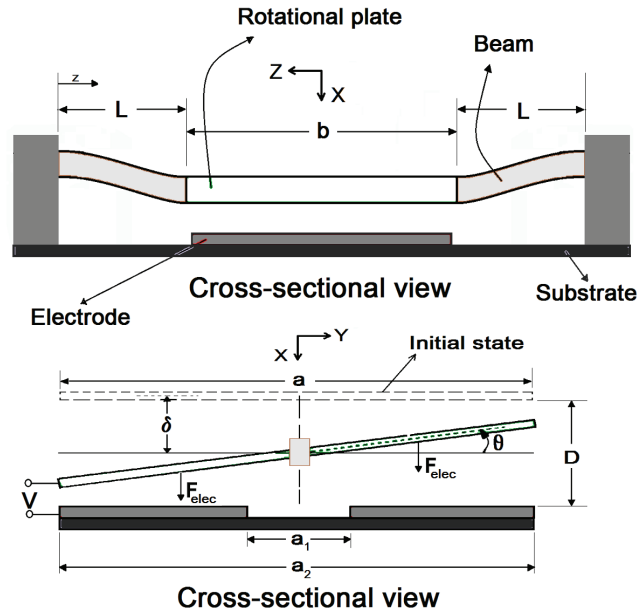


Fig. 1. Schematic diagram of electrostatic torsional actuator

One important issue which has a significant effect on instability behavior of torsional micro-actuators is coupling between the deflection and torsion response of the actuators. Most of the previous models considered only the torsion actuator. These approaches are acceptable if the vertical displacement of the movable electrode of the torsional actuator is very small. However, when the vertical displacement of the movable electrode is not negligible, the bending and torsion of the actuator are coupled. Degani and Nemirovsky [14] were the first researchers to introduce a lumped-mass model to capture the torsion/bending coupled behavior of torsional micro-actuators. Huang et al. [15] adopted this model to study the static behavior of a torsional micro-mirror. Daqaq et al. [16] investigated the nonlinear dynamic response of torsional micromirror using torsion/bending coupled model. More useful results can be found in Refs. [17, 18]

With reduction of dimensions from micro to sub-micro, nano-scale effects appear. One of the most important effects that appear at nano-scale dimensions is the size dependency of material characteristics. The size dependency is an inherent property of conductive metals when the characteristic size of the nano-structures is in the order of the internal material length scale. In this view, the size dependency of constitutive materials should be incorporated in modeling instability of NEMS [19, 20]. From a theoretical point of view, classical continuum mechanics are not capable of explaining the size-dependent behaviors of nano-structures. Therefore, non-classical continuum theories such as non-local elasticity [21], couple stress [22], modified couple stress theory [23] and augmented continuum mechanics [24, 25] are proposed to interpret the size-dependent behavior of nano-structures. The ability of augmented continuum mechanic in modeling the size dependent elastic properties of nano-structural elements such as nano-beams and nano-plates has been validated by comparing the theory with atomistic simulation [24, 25].

To the knowledge of the authors, none of the two mentioned issues (coupling effect and size effect) have contributed together in any pull-in models proposed by previous researchers. According to the wide applications of torsional nano-actuators, modeling the bending/torsion coupling and size effects seems to have great merits. Herein, the size dependent pull-in performance of torsional nano-actuator is investigated considering both coupling and size effects for the first time. The size dependent behavior of the constitutive material is modeled using non-classical augmented continuum theory. The coupling

between torsion and deflection has been incorporated in the model. The pull-in characteristics of the torsional actuator have been computed as basic design parameters.

2. PRELIMINARIES

Based on augmented continuum theory [24, 25], the elastic properties of nanoscale structural elements such as beams in flexural and torsion can be explained via surface energies. The effect of surface energies is significant when the length scale of the structure approaches several nanometers such as ultra-small NEMS. Previous researchers had utilized the surface energy concept to model the size dependent physical behavior of solids [26-28]. A brief elaboration on fundamentals of augmented continuum theory can be found in appendix A. Using augmented theory, the deviation of a general elastic property D from the conventional continuum theory D_c can be expressed as [24, 25]:

$$\frac{D-D_c}{D_c} = \alpha \frac{l}{h} \quad (1)$$

where α is a non-dimensional constant that depends on the geometry of the structural element, h is a length defining the size of the structure and l is a material length which sets the scale at which the effect of the free surfaces become significant. Assuming the cross-sectional width of a beam as the defining length of the actuator, Eq. (1) can be rewritten as (See appendix A):

$$\begin{aligned} (EI)_{eff} &= EI \left(1 + 8 \frac{l_b}{w} \right) && \text{for bending} \\ (GJ)_{eff} &= GJ \left(1 + 8 \frac{l_t}{w} \right) && \text{for torsion} \end{aligned} \quad (2)$$

where w is the cross-sectional width of a beam, E is Young's modulus, G is shear modulus, I is axial moment of inertia and J is polar moment of inertia. In the above relations, l_b and l_t are the bending and torsional material length scales, respectively. Note that for the torsion beams with a square cross-section, we have [29]:

$$I = \frac{w^4}{12} \quad \text{and} \quad J = \frac{w^4}{3} \left[1 - \frac{192}{\pi^5} \sum_{n=1}^{\infty} \frac{1}{(2n-1)^5} \tanh \left(\frac{(2n-1)\pi}{2} \right) \right] \quad (3)$$

Note that Relations (3) are valid for small deformation of rectangular cross-section, even for warped cross-sections.

3. THE GOVERNING EQUILIBRIUM EQUATION OF ELECTROSTATIC TORSIONAL ACTUATOR

Table 1 summarizes all the variables and definitions required for the analysis of the electrostatic torsional actuator. Three main assumptions used in this model are: 1) the torsion beams have perfect fixed boundary conditions around its axis. 2) The displacements of torsion beams are in small-deflection regime (including small vertical and angular displacements) until the pull-in occurs i. e., $\tan(\theta) \approx \sin(\theta) \approx \theta$, and $\cos(\theta) \approx 1$. This will give rise to less than 1% error, even at 10° [15]. 3) Any non-uniformity in the electric field due to the curvature and nonlinearity of the torsion/bending stiffness of the beams is ignored.

Table 1. A summary of all design variables for the electrostatic torsional actuator

E	Young's modulus of the torsion beam
ν	Poisson ratio of the torsion beam
$G = E/2(1 + \nu)$	Shear modulus of the torsion beam
b	Length of the mainplate
a	Width of the mainplate
L	Half length of the torsion beams
D	Gap between mainplate and electrode
w	Width of the torsion beam
a_1	Inner distance between two electrodes
a_2	Outer distance between two electrodes
V	Applied voltage between the mainplate and one electrode
θ	Torsion angle of the mainplate
δ	Vertical displacement of the mainplate
l_t	Torsional material length scales
l_b	Bending material length scales
$\alpha = a_1/a$	Normalized inner distance of the electrode
$\beta = a_2/a$	Normalized outer distance of the electrode
$\Theta = a\theta/(2D)$	Normalized torsion angle of the mainplate
$\Delta = \delta/D$	Normalized displacement of the manplate
I	Axial moment of inertia for the square cross-section
J	Polar moment of inertia for the square cross-section
K	Ratio of the bending to torsion stiffness' of the beam
$\bar{V} = V / (4GJ(2D)^3 / (Labe))^{1/2}$	Normalized applied voltage
\bar{V}_{cr}	Normalized pull-in voltage
Θ_{cr}	Normalized pull-in angle
Δ_{cr}	Normalized pull-in displacement

When the voltage is applied, the electrostatic attracting force arises between the electrode and mainplate. For a differential element of mainplate, this force can be written as [15]:

$$dF_{elec} = \frac{\epsilon V^2 b}{2(D - \delta - r \sin \theta)^2} dr \quad (4)$$

The total electrostatic force is given by integrating contributions of all the mainplate elements, hence

$$F_{elec} = \int_{\frac{a_1}{2}}^{\frac{a_2}{2}} dF_{elec} = \frac{\epsilon V^2 b}{2 \sin \theta} \left(\frac{1}{D - \delta - \frac{a_2}{2} \sin \theta} - \frac{1}{D - \delta - \frac{a_1}{2} \sin \theta} \right) \quad (5)$$

Similarly the electric moment of a differential element can be written as

$$dM_{elec} = \frac{\epsilon V^2 b}{2(D - \delta - r \sin \theta)^2} r dr \quad (6)$$

The total electrostatic moment about torsional axis is given by integrating contributions of all the mainplate elements, hence

$$M_{elec} = \int_{\frac{a_1}{2}}^{\frac{a_2}{2}} dM_{elec} = \frac{\varepsilon V^2 b}{2(\sin\theta)^2} \left(\frac{D-\delta}{D-\delta-\frac{a_2}{2}\sin\theta} - \frac{D-\delta}{D-\delta-\frac{a_1}{2}\sin\theta} + \ln \left(\frac{D-\delta-\frac{a_2}{2}\sin\theta}{D-\delta-\frac{a_1}{2}\sin\theta} \right) \right) \quad (7)$$

In order to develop the governing equation of the beams, the constitutive material of the nano-beam is assumed to be linear elastic and only the static deflection and rotation of the nano-beam is considered. When the actuator is driven to bend and rotate by the electrostatic force and torque simultaneously, an elastic recovery force and torque are generated from the bending and torsion of the nano-beams. These elastic resistances can be explained as the following relations:

$$F_{elas} = \frac{24EI}{L^3} \left(1 + 8 \frac{l_b}{w} \right) \delta$$

$$M_{elas} = \frac{2GJ}{L} \left(1 + 8 \frac{l_t}{w} \right) \theta \quad (8)$$

Now, note that the electrostatic actuation is balanced through the elastic resistance. Using Eqs. (5) (7) and (8), the static equilibrium equations of the system are derived as:

$$\frac{24EI}{L^3} \left(1 + 8 \frac{l_b}{w} \right) \delta = \frac{\varepsilon V^2 b}{2\sin\theta} \left(\frac{1}{D-\delta-\frac{a_2}{2}\sin\theta} - \frac{1}{D-\delta-\frac{a_1}{2}\sin\theta} \right) \quad (9)$$

$$\frac{2GJ}{L} \left(1 + 8 \frac{l_t}{w} \right) \theta = \frac{\varepsilon V^2 b}{2(\sin\theta)^2} \left(\frac{D-\delta}{D-\delta-\frac{a_2}{2}\sin\theta} - \frac{D-\delta}{D-\delta-\frac{a_1}{2}\sin\theta} + \ln \left(\frac{D-\delta-\frac{a_2}{2}\sin\theta}{D-\delta-\frac{a_1}{2}\sin\theta} \right) \right) \quad (10)$$

By applying $\sin(\theta) \approx \theta$ and using dimensionless parameters, Eqs. (9) and (10) can be rewritten using normalized parameter as

$$\Gamma_1(V, \theta, \Delta) = \bar{V} - \left(\frac{\left(1 + 8 \frac{l_t}{w} \right) \theta^3}{\left(\frac{1-\Delta}{1-\Delta-\beta\theta} - \frac{1-\Delta}{1-\Delta-\alpha\theta} + \ln \left(\frac{1-\Delta-\beta\theta}{1-\Delta-\alpha\theta} \right) \right)} \right)^{\frac{1}{2}} = 0 \quad (11)$$

$$\Gamma_2(V, \theta, \Delta) = \bar{V} - K \left(\frac{\left(1 + 8 \frac{l_b}{w} \right) \theta \Delta}{\frac{1}{1-\Delta-\beta\theta} - \frac{1}{1-\Delta-\alpha\theta}} \right)^{\frac{1}{2}} = 0 \quad (12)$$

Where $K = \left(\frac{3EIa^2}{GJL^2} \right)^{1/2}$, which is named the coupling ratio, physically explain the ratio of bending stiffness to torsion rigidity of the nano-beams (Coupling effect parameter). In the above relations, l reveals the size effect parameter. Equations (11) and (12) are the normalized equations representing a relationship between the torsion angle, vertical displacement, applied voltage, size effect and all the structural parameters of the actuator.

From Eqs. (11) and (12), it is obvious that the torsion angle and vertical displacement increase by applied voltage. When pull-in occurs, the applied voltage, the torsion angle and vertical displacement exceed their critical values (\bar{V}_{cr} , Θ_{cr} and Δ_{cr}) and the mainplate collapses abruptly.

The angle of rotation and vertical deflection of the mainplate can be calculated using the nonlinear Eqs. (11) and (12) at a given applied voltage. The pull-in state is found at the maximum of $\bar{V}(\Theta, \Delta)$. Using the implicit function theorem and Eqs. (11) and (12), to reach the maximum value of the $\bar{V}(\Theta, \Delta)$, the following equation should be satisfied:

$$\begin{vmatrix} \frac{\partial \Gamma_1(V, \Theta, \Delta)}{\partial \Theta} & \frac{\partial \Gamma_1(V, \Theta, \Delta)}{\partial \Delta} \\ \frac{\partial \Gamma_2(V, \Theta, \Delta)}{\partial \Theta} & \frac{\partial \Gamma_2(V, \Theta, \Delta)}{\partial \Delta} \end{vmatrix} = 0 \quad (13)$$

Solving Eqs. (11), (12) and (13) simultaneously, the pull-in voltage (\bar{V}_{cr}), angle of rotation (Θ_{cr}) and vertical deflection (Δ_{cr}) of the mainplate can be calculated.

4. RESULTS AND DISCUSSION

a) Neglecting size effect

Herein, the influence of coupling effect (K) on pull-in performance of a typical torsional nano-actuator with geometrical characteristics of $\alpha = 0.06$ and $\beta = 0.84$ is demonstrated, ignoring the size effect. Note that neglecting the size dependency is a common assumption in micro-structure literature.

Figure 2 shows the variation of pull-in angle as a function of coupling ratio for geometry of $\alpha = 0.06$ and $\beta = 0.84$. As seen, the torsion model (coupling neglected) predicts a certain value of pull-in angle of $\Theta_{cr} = 0.5236$ [15]. The pull-in angle of the nano-actuator decreases by decreasing the coupling ratio. On the other hand, Fig. 3 reveals that pull-in deflection of the actuator becomes considerable as K is reduced. Figure 4 shows the variation of pull-in voltage of the nano-actuator as a function of coupling ratio. Similar to what is observed for the pull-in angle, decreasing K leads to reducing the pull-in voltage from the value predicted by the torsion model ($\bar{V}_{cr} = 0.8365$). These findings can be interpreted via the diminishing bending stiffness of the system that results in softening the behavior of the nano-structure.

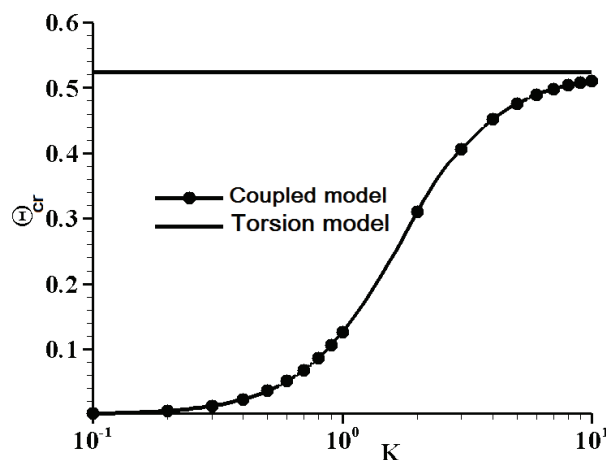


Fig. 2. Variation of pull-in angle vs. the electrode geometrical parameters for different K values

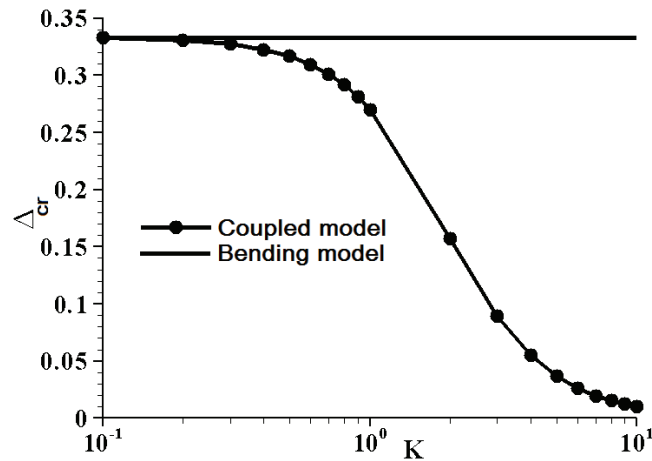


Fig. 3. Variation of pull-in displacement vs. the electrode geometrical parameters for different K values

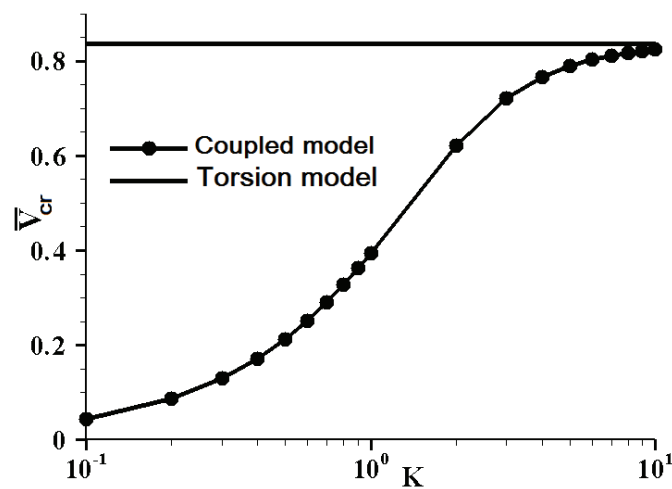


Fig. 4. Variation of pull-in voltage vs. the electrode geometrical parameters for different K values

b) Considering size effect

It should be noted that the sign of the material length scales depends on elastic constants (derivatives of strain energy tensor) of the materials [24, 25]. Hence, the sign and value of the material length scales of bulk metals generally depend on the crystallographic directions of the atoms. In many cases, while the bending material length scale of a square cross-sectional bar is often negative, torsional material length scale is usually positive [24, 25]. The effect of the variation of l_b and l_t on GJ and EI of square cross-sectional bar as a function of w are presented in Figs. 5a and 5b, respectively. As seen, while surface energy does reduce the bending stiffness of the actuator, it can provide a stiffening effect on torsion rigidity of the nano-structure.

For case study, consider a typical metal with material length scale characteristics of $l_b = -l_t$. Figures 6, 7 and 8, demonstrate the effect of size dependency on pull-in parameters for certain geometrical characteristics ($\alpha = 0.06$ and $\beta = 0.84$) and different K values. Variation of pull-in angle as a function of l/w has been demonstrated in Fig. 6. As seen, the increase in size effect decreases the pull-in angle of the actuator. On the other hand, size effect increases the pull-in deflection of the nano-actuator (Fig. 7). This effect is more significant for higher values of coupling ratio (K).

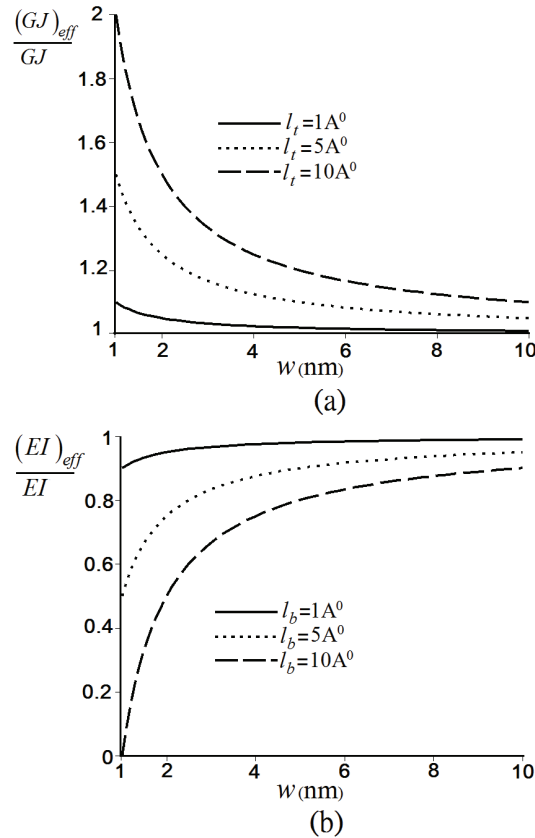


Fig. 5 Variation of (a) GJ and (b) EI of square cross-sectional bar as a function of w for different material length scales values

Figure 8 shows the influence of size effect on pull-in voltage of the torsional system. As seen from this figure, for very large values of coupling ratio (bending is negligible and torsion is dominant), decreasing the dimensions of nano-beams produces torsional hardening behavior of materials which leads to increase in the pull-in voltage of the actuator. On the other hand, for low values of coupling ratio (bending is dominant and torsion is negligible), decreases in the dimensions of nano-beams produce a bending softening behavior of materials, resulting in reduction of the pull-in voltage of the system. Interestingly, for a transient value of K , there is an increasing trend followed by further decreases in the pull-in voltage of the nano-structure (for example see $K=10$). Note that this enhancing-diminishing trend is the result of the superiority of the bending softening behavior of the material over the torsional hardening behavior.

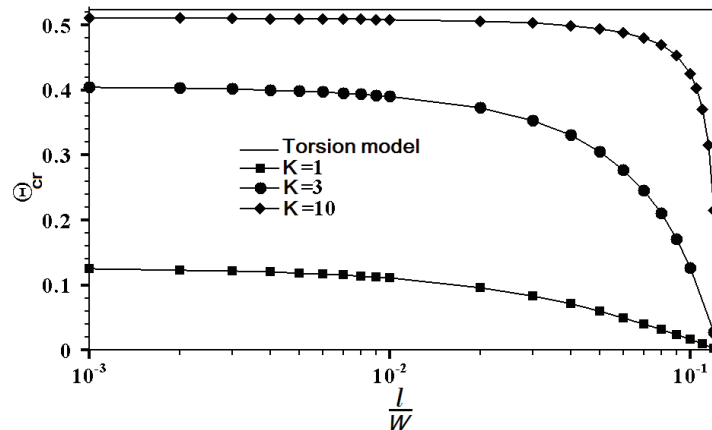


Fig. 6. Effect of size dependency on pull-in angle for different K values ($\alpha = 0.06$ and $\beta = 0.84$)

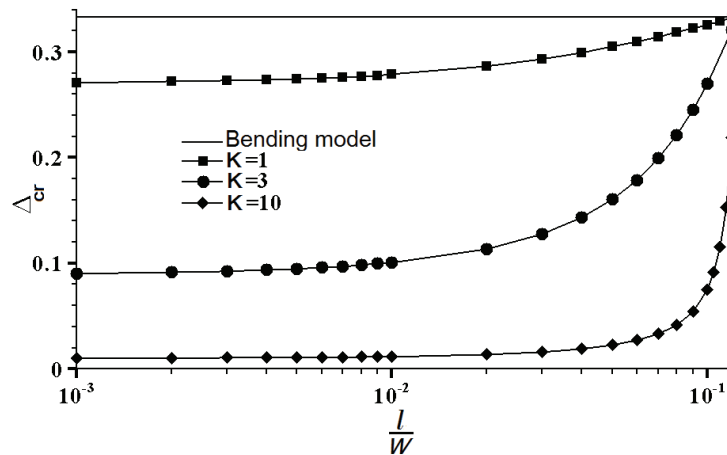


Fig. 7. Effect of size dependency on pull-in displacement for different K values ($\alpha = 0.06$ and $\beta = 0.84$)

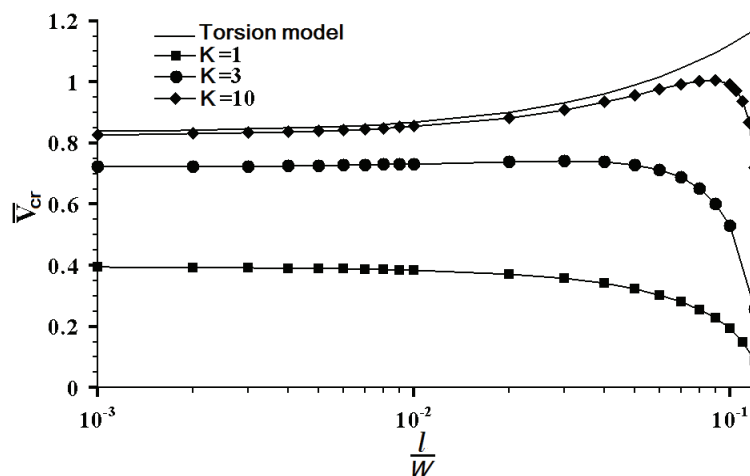


Fig. 8. Effect of size dependency on pull-in voltage for different K values ($\alpha = 0.06$ and $\beta = 0.84$)

Results of this section reveal that besides the bending/torsion coupling, the size dependency of materials is another important parameter that dominates the pull-in behavior of electrostatic torsional actuator. It is found that neglecting the size dependency and bending/torsion coupling in ultra-small actuators may cause major error during simulation of the system. This should be considered for modeling and designing nano-actuators.

5. CONCLUSION

Herein, effects of size dependency and bending/torsion coupling on static instability of torsional nano-actuator have been investigated. Augmented continuum mechanics in conjunction with Lagrangian multiplier solution method is utilized to model the size dependency of the actuator constitutive material. The static pull-in parameters are computed as a function of bending/torsion coupling ratio, actuator geometrical characteristics and size effect parameter. It is found that pull-in angle and voltage of the nano-actuator decreases by decreasing the in coupling ratio. On the other hand, pull-in deflection of the actuator becomes considerable as the coupling ratio is reduced. Results show that increasing in size effect decreases the pull-in angle of the actuator, whereas size effect increases the pull-in deflection of the nano-actuator (Fig. 7). This effect is more obvious for higher values of coupling ratio (K). Interestingly the effect of size dependency on pull-in voltage of the system greatly depends on coupling ratio and the superiority of bending mode over torsional mode. The findings of this work demonstrate the significant

influence of bending/torsion coupling and size effect on pull-in behavior of torsional actuators in nano-scales where the material length scale parameter is comparable with nano-structure dimensions. It is found that neglecting these effects in ultra-small actuators may cause comprehensive error in the simulation and design process.

REFERENCES

1. Saeidi, M. & Vaezzadeh, M. (2011). Theoretical investigation of the growth rate of carbon nanotubes in chemical vapor deposition. *Iranian Journal of Science & Technology, Transaction A: Science*, No. A1, pp. 29-32.
2. Mao, L. F. (2011). Study of the conduction band offset alignment caused by Oxygen vacancies in SiO_2 layer and its effects on the gate leakage current in nano-MOSFETs. *Iranian Journal of Science & Technology, Transaction of Electrical Engineering*, Vol. 35, No. E1, pp. 1-11.
3. Ghaffarpour Jahromi, S., Ahmadi, N. A., Mortazavi, S. M. & Vossough, S. (2011). Rutting and fatigue behavior of nanoclay modified bitumen. *Iranian Journal of Science & Technology, Transaction of civil Engineering*, Vol. 35, No. C2), pp. 277-281.
4. Sadrumontazi, A. & Fasihi, A. (2010). Influence of polypropylene fibers on the performance of nano- SiO_2 -incorporated mortar. *Iranian Journal of Science & Technology, Transaction B: Engineering*, Vol. 34, No. B4, pp. 385-395.
5. Zavracky, P. M., Majumber, S. & McGruer, E. (1997). Micromechanical switches fabricated using nickel surface micromachining. *J. Microelectromech. Syst.*, Vol. 6, pp. 3-9.
6. Ford, J. E., Walker, J. A. & Greywall, D. S. (1998). Goossen KW. Micromechanical fiber-optic attenuator with 3/spl mu/s response. *J. Lightwave Technol.*, Vol. 16, No. 9, pp. 1663-1670.
7. Toshiyoshi, H. & Fujita, H. (1996). Electrostatic micro torsion mirrors for an optical switch matrix. *J. Microelectromech. Syst.* Vol. 5, pp. 231-237.
8. Xiao, Z. X., Wu, X. T., Peng, W. Y. & Farmer, K. R. (2001). An angle-based design approach for rectangular electrostatic torsion actuators. *J. Microelectromech. Syst.*, Vol. 10, pp. 561-568.
9. Degani, O. & Nemirovsky, Y. (2002). Design considerations of rectangular electrostatic torsion actuators based on new analytical pull-in expressions. *J. Microelectromech. Syst.*, Vol. 11, pp. 20-26.
10. Nemirovsky, Y. & Degani, O. (2001). A methodology and model for the pull-in parameters of electrostatic actuators. *J. Microelectromech. Syst.*, Vol. 10, pp. 601-615.
11. Degani, O., Socher, E., Lipson, A., Leitner, T., Setter, D. J., Kaldor, S. & Nemirovsky, Y. (1998). Pull-in study of an electrostatic torsion microactuator. *J. Microelectromech. Syst.* Vol. 7, No. 4, pp. 373-379.
12. Zhang, X. M., Chau, F. S., Quan, C., Lam, Y. L. & Liu, A. Q. (2001). A study of the static characteristics of a torsional micromirror. *Sens. Actuators A*, Vol. 90, pp. 73-81.
13. Zhang, X. M., Chau, F. S., Quan, C., Lam, Y. L. & Liu, A. Q. (2001). Study of the static characteristics of a torsional micromirror. *J. Microelectromech Syst.*, Vol. 90, pp. 73-81.
14. Degani, O. B. & Nemirovsky, Y. (2001). Modeling the pull-in parameters of electrostatic actuators with a novel lumped two degrees of freedom pull-in model. *Sens. Actuat A*, Vol. 97-98, pp. 569-578.
15. Huang, J. M., Liu, A. Q., Deng, Z. L., Zhang, Q. X., Ahn, J. & Asundi, A. (2004). An approach to the coupling effect between torsion and bending for electrostatic torsional micromirrors. *Sens. Actuat A*, Vol. 115, pp. 159-167.
16. Daqaq, M. F., Abdel-Rahman, E. M. & Nayfeh, A. H. (2008). Towards a stable low-voltage torsional microscanner. *Microsyst Technol.*, Vol. 14, pp. 725-737.
17. Tadi Beni, Y., Abadyan, M. & Kochi, A. (2011). Effect of casimir attraction on torsion/bending coupled instability of electrostatic nano-actuators. *Physica Scripta.*, Vol. 84, 065801.

18. Rezazadeh, G., Khatami, F., Tahmasebi, A. (2007). Investigation of the torsion and bending effects on static stability of electrostatic torsional micromirrors. *Microsyst. Technol*, Vol. 13, pp. 715–722.
19. Abdi, J., Koochi, A., Kazemi, A. S. & Abadyan, M. (2011). Modeling the effects of size dependence and dispersion forces on the pull-in instability of electrostatic cantilever NEMS using modified couple stress theory. *Smart Mater. Struct.*, Vol. 20, 055011.
20. Tadi Beni, Y., Koochi, A. & Abadyan, M. (2011). Theoretical study of the effect of Casimir force, elastic boundary conditions and size dependency on the pull-in instability of beam-type NEMS. *Physica E*, Vol. 43, pp. 979-988.
21. Eringen, A. C. & Edelen, D. B. G. (1972). On nonlocal elasticity. *Int. J. Eng. Sci.*, Vol. 10, pp. 233–248.
22. Ejiike, U. B. C. O. (1969). The plane circular crack problem in the linearized couple-stress theory. *Int. J. Eng. Sci.*, Vol. 7, pp. 947–961.
23. Yang, F., Chong, A. C. M., Lam, D. C. C. & Tong, P. (2002). Couple stress based strain gradient theory for elasticity. *Int. J. Solids Struct.*, Vol. 39, pp. 2731–2743.
24. Miller, R. E. & Shenoy, V. B. (2000). Size-dependent elastic properties of nanosized structural elements. *Nanotechnology*. Vol. 11, pp. 139–147.
25. Shenoy, V. B. (2002). Size-dependent rigidities of nanosized torsional elements. *Int. J. Solids Struct.*, Vol. 39, pp. 4039–4052.
26. Gurtin, M. E. & Murdoch, A. I. (1975). A continuum theory of elastic material surfaces. *Archive for Rational Mechanics and Analysis*. Vol. 57, No. 4, pp. 291–323.
27. Rice, J. R. & Chuang, T. J. (1981). Energy variations in diffusive cavity growth. *Journal of the American Ceramic Society*, Vol. 64, No. 1, pp. 46–53.
28. Cammarata, R. C. (1994). Surface and interface stress effects in thin films. *Progress in Surface Science*, Vol. 46, No. 1, pp. 1–38.
29. Timoshenko, S. & Goodier, J. N. (1951). *Theory of elasticity*. New York: McGraw-Hill.

APPENDIX A: The fundamentals of augmented theory

According to the augmented theory [24], bulk stress tensor and surface stress tensor are denoted by σ_{ij} and τ_{ij} , respectively. The bulk stress tensor satisfies the equilibrium equation (with no body force)

$$\sigma_{ij,j}=0 \quad (A1)$$

Equilibrium of surface tensor necessitate that

$$\tau_{ij,j} + f_i = 0, \quad \tau_{ij} \kappa_{ij} = \sigma_{ij} n_i n_j \quad (A2)$$

where n_i is the normal to the surface, f_i is the component of the traction $\sigma_{ij} n_j$ along the i direction along the surface and κ_{ij} is the curvature tensor (which vanishes in the present set up). Surface effects introduce an additional force per unit length around the edges of the cross section. This force is due to the surface stresses introduced during bending. These forces can be found from the strains to be

$$F = S \varepsilon_{11} = \frac{-Sy}{\rho} \quad (A3)$$

where y is the distance from the centerline of the cross section and ρ is radius of curvature. The quantity of S is the surface elastic constant relevant to the structural element being considered. By applying the force from surface effect, the moment balance leads to

$$M = \int_A \sigma_{11} y dA + \int_{\partial A} F y dl = \frac{-1}{\rho} \left(EI + S \int_{\partial A} y^2 dl \right) = \frac{-1}{\rho} (EI + SQ) \quad (A4)$$

where

April 2012

IJST, Transactions of Mechanical Engineering, Volume 36, Number M1

$$Q = \int_{\partial A} y^2 dl \quad (\text{A5})$$

Comparing the equation above, we recognize the quantities of interest to be $D_c = EI$ and $D = EI + SQ$ and thus

$$\frac{D - D_c}{D_c} = \frac{S}{E} \frac{Q}{I} \quad (\text{A6})$$

For the square beams, we find $I = w^4/12$ and $Q = 2w^3/3$. Using these results in Eq. (A6) we obtain

$$\frac{D - D_c}{D_c} = 8 \frac{S}{E} \frac{1}{w} = 8 \frac{l_b}{w} \quad (\text{A7})$$

If we use $D_c = EI$ and $D = (EI)_{eff}$, Eq. (A7) is written as

$$(EI)_{eff} = EI \left(1 + 8 \frac{l_b}{w} \right) \quad (\text{A8})$$

According to the theory of torsion based on the augmented theory of reference [25] the torsion problem of bar can be formulated as

$$\begin{cases} \nabla^2 \Psi = -2 \\ \Psi + 2 \frac{l_t}{w} \frac{\partial \Psi}{\partial n} = 0 \end{cases} \quad (\text{A9})$$

where

$$\Psi = \frac{\psi}{(w/2)^2}, \quad \xi = \frac{x_2}{w/2}, \quad \eta = \frac{x_3}{w/2} \quad (\text{A10})$$

where ψ is stress function and x_2 and x_3 are coordinates of every point in the cross section of bar. The rigidity of bar during the torsion is defined as

$$\frac{D}{G(w/2)^4} = 2 \int \Psi d\xi d\eta \quad (\text{A11})$$

Using perturbation method [25], the solution of Eq. (A9) can be rewritten as

$$\Psi = \Psi + \left(\frac{2l_t}{w} \right) \Psi_1 + \left(\frac{2l_t}{w} \right)^2 \Psi_2 + \dots \quad (\text{A12})$$

According to the stage of the above solution, the following relation can finally be obtained to explain the surface effect on the torsional rigidity of beam

$$\frac{D - D_c}{D_c} \approx \frac{A_1}{A_0} \frac{2l_t}{w} \quad (\text{A13})$$

After some computations the coefficients A_0 and A_1 are computed as [25]

$$A_0 = 2.2492, \quad A_1 = 8.9969 \quad (\text{A14})$$

If we use equation (A13) and $D_c = GJ$ and $D = (GJ)_{eff}$ Eq. (A13) can be rewritten as

$$(GJ)_{eff} = GJ \left(1 + 8 \frac{l_t}{w} \right) \quad (\text{A15})$$